Available online at www.sciencedirect.com
SCIENCE DIRECT®
C. R. Physique 6 (2005) 595–603
COMPTES RENDUS PHYSIQUE
http://france.elsevier.com/direct/COMREN/

Interaction of electromagnetic fields with the environment/Interaction du champ électromagnétique avec l'environnement

A geometrical optics and uniform theory of diffraction based ray tracing optimisation by a genetic algorithm

Romain Matschek

Ministère de l'Intérieur et de l'Aménagement du Territoire, 7, rue des Campanules, 77185 Lognes, France

Available online 30 August 2005

Abstract

Lack of knowledge of the material properties (medium, thickness, structure, roughness, ...) has a strongly negative impact on the quality of the radioelectric field predictions obtained by rigorous methods. In order to be able to optimise our model based on Geometrical Optics (GO) and Uniform Theory of Diffraction (UTD)—exploiting the rays obtained by a three-dimensional ray tracing (combining reflection, transmission and diffraction)—we associate a genetic algorithm (GA) to it. We evaluate their performances after optimisation on a typical indoor environment, and then we determine the influence of a few ray tracing parameters on the prediction accuracy and thus the knowledge of the environment of simulation. ***To cite this article: R. Matschek, C. R. Physique 6 (2005).***

Résumé

Optimisation par un algorithme génétique d'un modèle basé sur l'optique géométrique et la théorie uniforme de la diffraction. La méconnaissance des caractéristiques des matériaux (nature, épaisseur, structure, rugosité, ...) est fortement préjudiciable à la qualité des prédictions du champ radioélectrique obtenu par des méthodes rigoureuses. De façon à pouvoir optimiser notre modèle basé sur l'Optique Géométrique et la Théorie Uniforme de la Diffraction exploitant les rayons obtenus par un tracé de rayon tridimensionnel (combinant réflexions, transmissions et diffractions), nous lui avons associé un algorithme génétique. Nous en avons évalué les performances après optimisation sur différents environnements indoor, et nous avons ensuite déterminé l'influence des différents paramètres du tracé de rayons sur l'acuité des prédictions et donc la connaissance de l'environnement de simulation. ***Pour citer cet article : R. Matschek, C. R. Physique 6 (2005).***

Keywords: Ray tracing; Geometrical Optics; Uniform Theory of Diffraction; Indoor; Genetic algorithm

Mots-clés : Tracé de rayons ; Optique Géométrique ; Théorie Uniforme de la Diffraction ; Indoor ; Algorithme génétique

1. Introduction

Having an accurate tool to predict the electromagnetic field in varied environments (indoor and urban) in a wide frequency bandwidth is an imperative condition to deploy correctly mobile networks, Wifi hot-spots, etc.

This tool must realise a compromise between computational time and accuracy to ensure compatibility with operational constraints of engineering. It then requires a good knowledge of the environment: the modelling of the calculation scenes'

E-mail address: romain.matschek@wanadoo.fr (R. Matschek).

1631-0705/$ – see front matter
doi:10.1016/j.crhy.2005.07.001

geometry is a paramount factor of the prediction quality, but the intrinsic characteristics of materials constitutive of these scenes are also important, especially when simulations are based on physical models.

Taking into account the currently used frequencies for high data rate radio communications (from approximately 500 MHz up to 100 GHz) and of the required accuracy (standard deviation of about 6 to 8 dB), we developed a tool combining a three-dimensional ray tracing with a model based on Geometrical Optics (GO) and Uniform Theory of Diffraction (UTD); it will be presented in a first part.

It appeared to us that the intrinsic characteristics of materials given in the literature are not suitable to obtain systematically predictions of a satisfactory quality; in a second part, we will thus describe the genetic algorithm (GA) implemented in our tool in order to carry out a multivariable optimisation (relative permittivity, conductivity, thickness, even roughness, for about ten materials and thus about fifty unknown factors). Finally, in a last part, we will compare some simulations given by our tool to electromagnetic measurements realised in an indoor environment, by analysing the convergence of the algorithm and the influence of the rays on the performance of the radioelectric predictions.

2. Context

2.1. Environment

A calculation scene is the combination of data resulting from a Geographical Information System (ground, vegetation, etc.) and from architecture software (for buildings), eventually completed by specific elements (furniture, etc.). This information is indicated in the form of plane facets made up of an unspecified number of points. The edges must have dimensions compatible with the frequency of simulation: in the case of our model based on GO, we regard as valid any edge of size higher than approximately 10λ. Some examples of such scenes are given in Fig. 1.

2.2. Materials

In the following, we will assume that the materials are homogeneous, linear and isotropic, and the relative permeability will be equal to unity.

Dielectrics could be lossy, provided that the conductivity is such that the loss angle is lower than a few percents (in the contrary case, the index of refraction is strongly complex and the phase and amplitude plans are then dissociated, giving an inhomogeneous wave making null and void the ray approach [1]).

In this paper, roughness will not be taken into account.

2.3. Radioelectric parameters

The higher the frequency, the more valid the optical approach (resulting from the locality principle) [2]; frequency bandwidth of a tool based on GO and UTD is thus very wide, with the following restrictions:

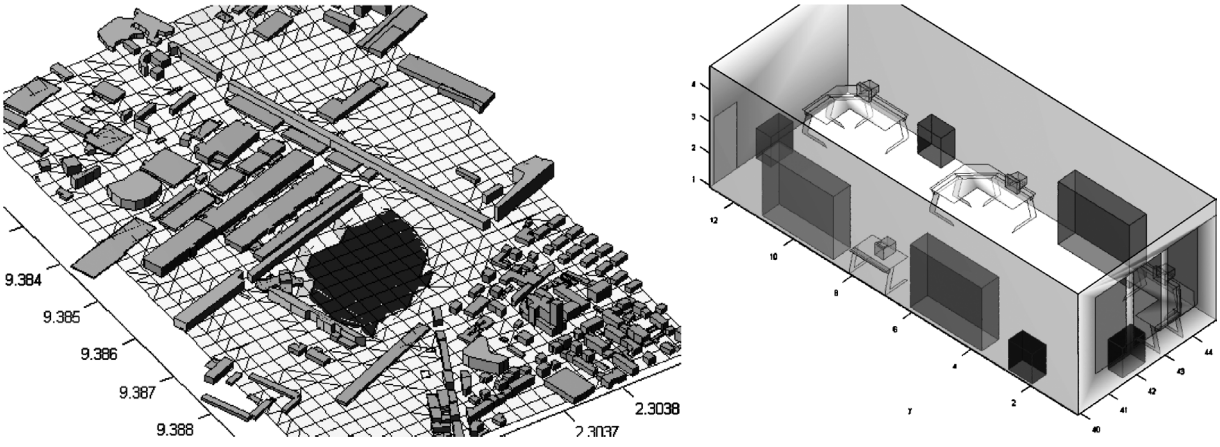

Fig. 1. Examples of calculation scenes (on the left: outdoor; on the right: indoor).

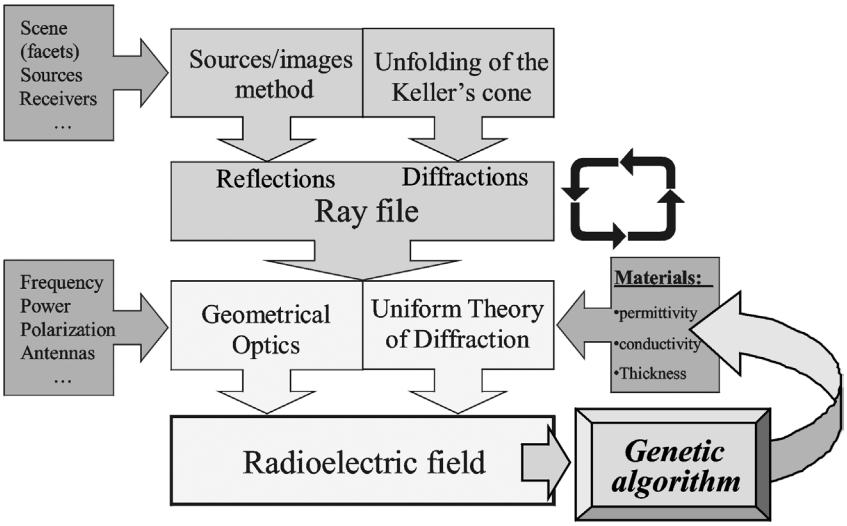

Fig. 2. The simulation tool.

- The lowest frequency depends on the dimension of the facets (cf Section 2.1) and the distances between the points of emission and reception (if k is the wave number and L the distance parameter used in UTD—cf. Section 4.2, one must have $k \cdot L \gg 1$) [3].
- The wavelength is much larger than the size of roughnesses [4].

The wave resulting from the source is regarded as spherical, unconstrained on its polarisation; in the same way, antenna diagrams (with the emission as with the reception) could be unspecified.

2.4. Simulations

The tool used here is based on two main components:

- the ray tracing which, starting from geometrical information on the scene and the points of emission and reception, finds valid geometric paths including several reflections, transmissions and diffractions, which are next stored in a ray file (this is described in Section 3),
- using the ray file, the materials, the characteristics of the sources and the receivers, the calculation model of the radioelectric field calculates the vector field in amplitude and phase (described in Section 4).

The main components of our tool are summarized in Fig. 2.

3. The ray tracing

3.1. Direct, reflected and transmitted rays

Direct and transmitted rays are obtained by a rectilinear tracing followed by a test of screening [5]. To look for reflected rays, we use the traditional method of sources/images.

3.2. Diffracted rays

Finding multiple diffractions is significantly more complex than that of the other interactions, in particular when the various phenomena (reflection, transmission and diffraction) are combined.

The application of the principle of locality and the generalised Fermat [6] principle to the case of diffraction makes it possible to define a cone—known as *Keller's cone*—giving the potential directions of the diffracted rays, as illustrated by Fig. 3 [7].

To find the path of a ray undergoing N diffractions (without reflections), we thus assume that an edge i is defined by its origin point $\vec{s}_i$ and a vector $\vec{r}_i$ giving its orientation and its length [8].

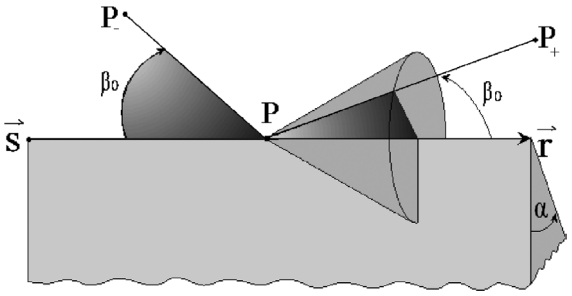

Fig. 3. Keller's cone.

If a_i is a scalar ranging between 0 and 1, an unspecified point of edge i can thus always be defined by:

$$\vec{P}_i = a_i.\vec{r}_i + \vec{s}_i \tag{1}$$

For each point of diffraction we have thus to solve, if suffixes '$-$' and '$+$' denote respectively the 'back' and 'forward' points and β_0 is the diffraction angle:

$$\cos(\beta_0) = \frac{\vec{P}_+ - \vec{P}}{\|\vec{P}_+ - \vec{P}\|}.\frac{\vec{r}}{\|\vec{r}\|} = \frac{\vec{P} - \vec{P}_-}{\|\vec{P} - \vec{P}_-\|}.\frac{\vec{r}}{\|\vec{r}\|} \tag{2}$$

By developing this expression for each diffraction, we get a system of non-linear equations whose resolution is immediate with the first order, and simple to the second order (with the Newton–Raphson method for example).

To combine reflections with diffractions, we applied the method of the sources/images (cf. Section 3.1) to the diffracting edges, such that the previously exposed case for diffractions only is applicable.

The ray tracing algorithm integrates an original classification of the edges making it possible to eliminate the non-causal solutions (images of the same order but not resulting from the same facets).

4. Radioelectric field computation

The ray file generated by the tracing contains the type and the position of the impacts constituting of the optical path between a source and a point of observation, and various geometrical parameters of the scene (wedge apertures, angles of reflection or diffraction, etc.). With this information, it is then possible to predict the received field by applying GO laws and the UTD formulation which was the subject of many publications (with a particular mention for [2] and [3]) and will be only briefly presented in this section.

4.1. Geometrical Optics

Along the optical path, the radioelectric field is affected by a variation of phase and a variation of amplitude related to the spreading factor of the beam $A(s)$ at the distance s from the source E^0.

If k is the wave number, one can then express the variations of the field E^s due to the propagation of the ray:

$$E^s = E^0 \cdot A(s) \cdot \mathrm{e}^{-j\cdot k\cdot s} \quad \text{where } A(s) = \frac{1}{s} \text{ for spherical waves} \tag{3}$$

When the ray undergoes a reflection R or a transmission T, the field is also affected by a Fresnel coefficient depending on the angle of incidence Ψ, the complex relative permittivity $\hat{\varepsilon}_r$ and the polarisation s (*soft* $\equiv E_\perp$) or h (*hard* $\equiv E_\parallel$). These coefficients are expressed below:

$$R^{s,h}(\psi) = \frac{\xi^{s,h}\cdot\sin\psi - \sqrt{\hat{\varepsilon}_r - \cos^2\psi}}{\xi^{s,h}\cdot\sin\psi + \sqrt{\hat{\varepsilon}_r - \cos^2\psi}} \quad \text{and} \quad T^{s,h}(\psi) = \frac{2\cdot\sqrt{\xi^{s,h}}\cdot\sin\psi}{\xi^{s,h}\cdot\sin\psi + \sqrt{\hat{\varepsilon}_r - \cos^2\psi}} \quad \text{with } \begin{cases}\xi^s = 1\\ \xi^h = \hat{\varepsilon}_r\end{cases} \tag{4}$$

4.2. Uniform Theory of Diffraction

From the exact resolution of the canonical case of the infinite metallic half-plane (Sommerfeld's solution), it is possible to obtain a heuristic formulation ([7] then [9]) allowing the calculation of the field diffracted by a lossy dielectric wedge [10].

If Q is the point of diffraction, s' is the distance from the source to this point and s is now the distance between Q and the point of observation, the diffracted field can then be expressed:

$$\vec{E}^d(P) = \vec{E}^i(Q) \cdot \overline{\overline{D}}^{s,h} \cdot A(s,s') \cdot \mathrm{e}^{-j\cdot k\cdot s} \tag{5}$$

where the spreading factor A, in the case of a spherical wave, is given by:

$$A(s,s') = \sqrt{\frac{s'}{s(s+s')}} \tag{6}$$

$\overline{\overline{D}}^{s,h}$ is a 2nd order tensor whose coefficients, expressed below, depend on polarisation (suffixes 0 and n of the reflection coefficients indicate the 2 faces of the wedge):

$$D^{s,h} = D_1 + D_2 + R_n^{s,h} \cdot D_3 + R_0^{s,h} \cdot D_4 \tag{7}$$

With [11,12]:

$$D_m = \frac{-\mathrm{e}^{-j\pi/4}}{2n\sqrt{2\pi k_0}\cdot \sin\beta_0'} \cdot \cot\left[\frac{\beta_m}{2n}\right] \cdot F\left[k\cdot L\cdot \sin^2\left(\frac{\beta_m}{2n}\right)\right], \quad m = \{1,\ldots,4\} \tag{8}$$

where β_m is an angle related to the optical boundaries (existence of the incident and reflected rays compared to the two faces of the wedge), and β_0' is the angle between the incident ray and the edge. F is the Fresnel function expressed by:

$$F(x) = 2\cdot j\cdot \sqrt{x}\cdot \mathrm{e}^{jx} \cdot \int_{\sqrt{x}}^{\infty} \mathrm{e}^{-ju^2}\,\mathrm{d}u \tag{9}$$

L is the distance parameter which guaranties the continuity of the field near the boundaries and n is a function of the angle of aperture α; they are defined by [13]:

$$L = \frac{s\cdot s'\cdot \sin\beta_0'}{(s'+s)} \quad \text{and} \quad n = \frac{(2\pi-\alpha)}{\pi} \tag{10}$$

Multiple refinements were introduced into UTD to extend its field of application, often in a heuristic way; we will not evoke them here but one will be able to consult with benefit the examples detailed in the following references: improvement of the UTD diffraction coefficients [14], diffraction of an inhomogeneous plane wave by a wedge [15,16], complex penetrable wedge [17], UTD heuristic formulation to take into account a transmitted ray through a lossy dielectric wedge [18,19].

Let us, however, note that when the ray diffracted by an edge is again diffracted by another edge of the same facet (inducing a grazing incidence), it is necessary to take into account the slope diffraction [20]. The total diffracted field is then expressed, if φ' is the angle of incidence [2,3]:

$$E^d(P) = \left[E^i(Q)\cdot D^{s,h} + \frac{1}{jk}\cdot \frac{\partial D^{s,h}}{\partial \varphi'} \cdot \frac{\partial E(Q)}{\partial n}\right] \cdot A(s,s') \cdot \mathrm{e}^{-j\cdot k\cdot s} \tag{11}$$

4.3. Knowledge of the materials

With a 3D ray tracing and an accurate model for predicting the radioelectric field, it is now possible to carry out simulations as well indoor as outdoor, in so far as the constraints clarified in Sections 2.2 and 2.3 are respected. It is though necessary to know precisely the intrinsic characteristics of materials.

The literature is abundant on this subject; we present for example in Table 1 the values recommended by the COST 231 [21] for losses in building materials, in the band 1–2 GHz.

However, it is important to precise that, on the one hand, the precision of the predicted field strongly depends on the material characteristics and that, on the other hand, those have a strong variability. In addition, the structure of materials (multiple layers, roughness, etc.) cannot be systematically observed and modelled. Lastly, it seems unrealistic to seek to characterise these materials in situ (expensive and delicate measurements, in addition not easy to extrapolate) [22]. We thus chose to optimise materials starting from radioelectric measurements of reference. Optimisation to be realised must be multivariable but not sensitive to local minima.

For these two constraints, a genetic method seemed to be useful. Indeed, this technique is largely used in many domains, for example in electromagnetics for antenna diagrams optimisation.

Table 1
Typical losses in the band 1–2 GHz

Context	Material	Losses
Outdoor	Thick concrete wall (25 cm)	13
	Reinforced glazing	8
Indoor	Thin concrete wall (< 10 cm)	6
	Pave	23
	Brick	2.5
	Plasterboard	1.5
	Windows	2

5. The genetic algorithm

5.1. Principle

Based on mechanisms derived from the life observation [23], a GA makes it possible to find a quasi optimal solution of a multivariable problem; largely based on random numbers, this algorithm will converge more or less quickly and more or less effectively with each pulling.

We will call *gene* the set of the materials constituting a calculation scene. Several genes will be combined together, thus constituting a *population* which will evolve several times. Our GA is integrated in the prediction tool at the electromagnetic model level, without requiring any change of the existing ray file, as illustrated on Fig. 2. Its successive iterations thus generate a reasonable computing time, by refining only the parameters related to materials without impairing the rigour of the optical methods used.

5.2. Implementation

The coding of the genes (i.e., of materials) depends on the limit values of the several variables and the desired granularity; our choice is illustrated in Fig. 4. P_m is the change probability of the gene; the relative permittivity ε_r, the conductivity σ and the thickness e of a material are then obtained by (A, B, C and D refer to Fig. 4):

$$\begin{cases} \varepsilon_r = \frac{A}{40} + 1 \\ \sigma = 10^{\frac{B}{100}-7} \\ e = C \text{ (mm)} \\ p_m = 10^{-D-1} \end{cases} \Rightarrow \begin{cases} \varepsilon_r = [1 \dots 13,775] \\ \sigma = [10^3 \dots 10^{-7}] \\ e = [0 \dots 1023 \text{ mm}] \\ p_m = [10^{-8} \dots 10^{-1}] \end{cases} \tag{12}$$

The GA evolves according to several steps: initialisation of the population, evaluation of various genes, selection of best genes, crossing of the genes with 1 or 2 points, random mutation, convergence test, and new iteration or writing of the new material file.

During initialisation, a gene carries the information contained in the initial material file; the other genes are initialised in a completely arbitrary way.

The evaluation consists in calculating the error induced by each gene by comparing the field predicted with a reference field. Various formulas can be used, according to whether one wants to reduce the standard deviation of the error, to reduce its

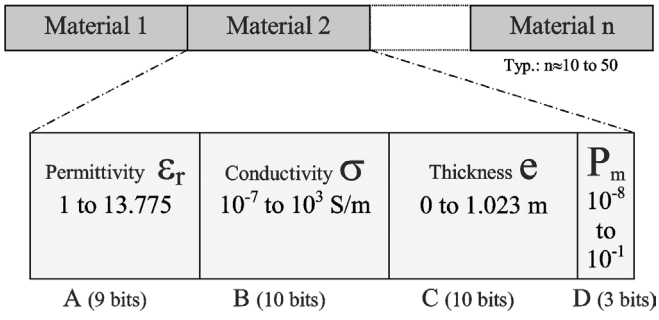

Fig. 4. The gene.

average, to minimise the error relative to strongest fields, etc. In addition, one can calculate this error starting from the fields expressed into linear or into dB. We chose to implement the following expression:

$$error = \frac{1}{\text{nb receivers}} \cdot \sum_{i=1}^{\text{nb receivers}} \left(\left| \log_{10} \left\{ \frac{(E^{\parallel}_{\text{predicted}_i})^2 + (E^{\perp}_{\text{predicted}_i})^2}{(E^{\parallel}_{\text{reference}_i})^2 + (E^{\perp}_{\text{reference}_i})^2} \right\} \right| \right) \tag{13}$$

The selection makes it possible to choose the best genes (i.e., those which present the best adaptation); a compromise must be carried out between the will to converge and the need for guaranteeing the population a certain genetic diversity. We chose to preserve 10% of the best genes. The 90% of genes not preserved are then generated by crossing over two by two the previous genes classified according to their adaptation.

Randomly, the crossing is done at 1 or 2 points, the position of the points of cut being also random.

Finally, random binary errors are introduced in the genes, making it possible to keep diversity in the population and also exploring solutions impossible to generate by crossover. In our implementation, the probability of mutation moreover is self-managed by the algorithm itself.

6. Results

6.1. Reference measurements

We chose to test our prediction model and its associated GA on an indoor configuration (inducing a reasonable time to find the rays). The calculation scene is a recent building of 6 floors. A source emits at 1.8 GHz on the 2nd floor, and reference measurements are realised at the 1st floor. Both transmitter and receiver antennas are omnidirectional ones, in vertical polarisation.

Let us notice that the choice of a building configuration is de facto penalising, not only because of the presence of a slab of armed concrete between the floors, but also because the surrounding buildings were deliberately not integrated into the calculation scene. This is represented in Fig. 5 (on the left).

Over 500 iterations, the GA converges quickly, then requires the mediation of the mutations (which make fall the average value) to continue to progress; in fact, the GA converges in stages.

Indeed, various uncertainties relative to the scene (geometry, modelling, materials, etc.) and to the source (emitted power, antenna diagram, polarisation, orientation, specific disturbers, etc.) seldom allow a perfect convergence, independently of any consideration on the validity of the method used (GO and UTD).

After optimisation, the error between prediction and measurements gives an average of 1.71 dB and a standard deviation of 6.73 dB. Let us recall that the choice of the function of evaluation advantages the decrease of the standard deviation and not that of the average, which explains why it is quite significant.

Note also that optimised values for the several materials of the scene are quite different from those usually used in simulations (some measurements of concrete around 2 GHz [22] gave a relative permittivity of 6.56 and a conductivity of 1 $\text{mS}\cdot\text{m}^{-1}$). Table 2 shows the optimised values for the 1st floor illustrated in Fig. 5.

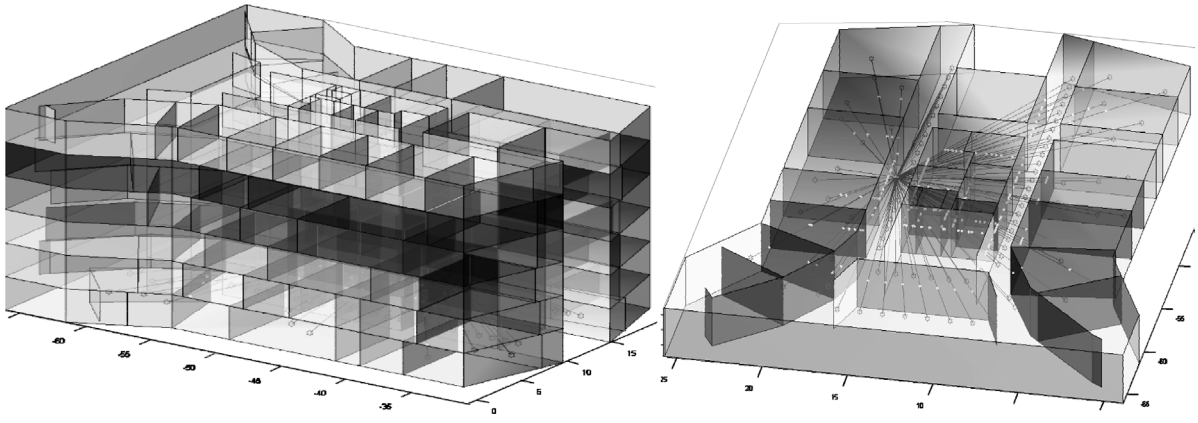

Fig. 5. The indoor scene (on the left: complete, for optimisation; on the right: the 1st floor, for validation).

Table 2
Optimised values for the 1st floor at 1.8 GHz

Material	Thickness (cm)	Relative permittivity	Conductivity ($mS \cdot m^{-1}$)
Thick concrete wall	32.2	12.1	0.11
Partition	63(!)	8.1	3.10^{-4}
Lower pave	27.5	1.6	21.38
Upper pave	63.5	10.9	1000 (non-penetrable)

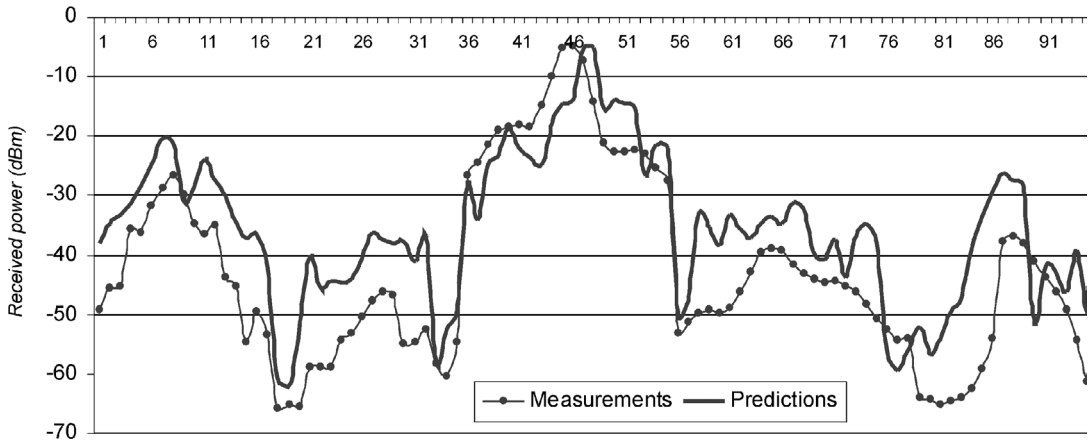

Fig. 6. Comparison simulation/measurements.

6.2. Comparison predictions/measurements

To evaluate our intrinsic characteristics, we will now compare the predictions given by our model to measurements realised on the 2nd floor (the transmitter remains unchanged at the 2nd floor). The set of materials is then a subset of that optimised previously. The new calculation scene is illustrated on the right of Fig. 5 (with rays, reception points, reflection, transmission and diffraction points).

Comparison between simulations (bold line) and measurements (line with circles) is illustrated in Fig. 6 (received power in dBm for 96 points of measurements). The standard deviation of the error is now 7.69 dB and the average falls to 7.2 dB.

6.3. Comments

In spite of the fact that the standard deviation remains acceptable (by comparison to that of other indoor propagation models), these statistics show that the scene was not sufficiently detailed. Transmitted rays through the partitions of the 1st stage result in an excessive predicted field, attesting that these partitions have been regarded by our model as bringing less attenuation than actually happens. In other words, a significant contribution of the measured field did not result from the 162 rays found by the ray tracing during optimisation. This remark suggests in particular to take into account the roughness in our model, in order to introduce a certain dispersion of energy (reduction of the specular contribution of the reflections).

In addition, it is important to notice that the ray tracing settings is more demanding for the test set than for optimisation (3 phenomena to the maximum); we indeed authorised a more significant number of phenomena per ray, in particular concerning the transmissions. This point is essential because it illustrates the flexibility brought by the choice to rather optimise the materials than the electromagnetic model (contrary to the semi-empirical approaches which are then related to the environment of reference).

It should, however, be noted that the richer the ray file will be, the more the computed field will depend on materials, the phenomena and the angles of incidence, thus supporting the quality of the optimisation carried out by GA. Observation of the Fresnel coefficients (cf. Eq. (4)) lets us suppose that the transmissions depend primarily on conductivity, whereas the relative permittivity mainly influences the reflections.

Lastly, let us remark that GA is very powerful in computational time: the results exposed here having been obtained in a few minutes on a relatively standard PC (Pentium IV, 2 GHz). Moreover, this computational time, by the principle of the algorithm, increases linearly with the number of unknown factors whereas, by other methods of optimisation, this increase is often quadratic.

7. Conclusion

In order to be able to predict the electromagnetic field in varied environments for a wide frequency bandwidth, a tool associating a ray tracing and a model based on GO and UTD was presented. First, the combined research of the various phenomena taken into account (reflection, transmission, diffraction) was presented; then, GO and UTD were briefly detailed.

The knowledge of the intrinsic characteristics of materials is of primary importance for accurate predictions; after having noted that the values given in the literature were not sufficiently accurate, we presented the GA implemented in our tool for carrying out the optimisation of these characteristics, starting from measurements of radioelectric field. The coding of gene, the error function and the various parameters of this GA were specified. The global performance of the tool (ray tracing associated to radioelectric model) was finally evaluated to real indoor measurements.

Once optimised, this model presents an accuracy equivalent to that of other more traditional models (semi-empirical, etc.), but with a higher adaptivity.

With the intrinsic characteristics of materials optimised by the tool, the optical methods thus seem completely adapted to the prediction of electromagnetic field in varied environments, in so far as their representation is sufficiently precise (geometry, type of material and positioning).

Acknowledgements

This work was partially completed in France Telecom Recherche & Développement, Belfort. The author would like to thank the radio laboratory for its indoor measurements, and the R&D engineers who have supported this work.

References

[1] J. Lavergnat, M. Sylvain, Propagation des ondes radioélectriques, Collection Pédagogique des Télecommunications, Masson, Paris, 1997.
[2] G.L. James, Geometrical Theory of Diffraction for Electromagnetic Waves, Peter Peregrinus, UK.
[3] D.A. McNamara, C.W.I. Pistorius, J.A.G. Malherbe, The Uniform Geometrical Theory of Diffraction, Artech House, London, 1990.
[4] J.-F. Legendre, Etude de modèles de prédiction de la propagation basés sur la Théorie Géométrique de la Diffraction, PhD Thesis, INSA, Rennes, 1995.
[5] A.S. Glassner (Ed.), An Introduction to Ray Tracing.
[6] M. Born, E. Wolf, Principles of Optics, Pergamon Press, Elmsford, NY.
[7] J.B. Keller, Geometrical theory of diffraction, J. Opt. Soc. Amer. 52 (2) (1962) 116–130.
[8] T. Imai, T. Fujii, Propagation Loss in Multiple Diffraction Using Ray-Tracing, IEEE AP, 1997.
[9] R.G. Kouyoumjian, P.H. Pathak, A uniform geometrical theory of diffraction for an edge in a perfectly conducting surface, Proc. of the IEEE 62 (11) (1974) 1448–1461.
[10] R.J. Luebbers, A heuristic UTD slope diffraction coefficient for rough lossy wedges, IEEE Trans. Ant. Prop. 37 (2) (1989) 206–211.
[11] P.D. Holm, UTD-diffraction coefficients for higher order wedge diffracted fields, IEEE Trans. Ant. Prop. 44 (6) (1996) 879–888.
[12] Y. Liu, R. Ciric, Improved formulas for the diffraction by a wedge, Radio Science 28 (5) (1993) 859–863.
[13] P. Mariage, P. Fiorot, P. Degauque, Amélioration de la théorie uniforme de la diffraction appliquée de manière conventionnelle à la double diffraction par des dièdres joints ou disjoints dans les régions de recouvrement des zones de transition, Ann. Telecommun. 53 (9–10) (1998).
[14] H. El-Sallabi, P. Vainikainen, Improvement in heuristic UTD diffraction coefficient, Electron. Lett. 39 (1) (2003) 10–12.
[15] H.L. Bertoni, A.C. Green, L.B. Felsen, Shadowing an inhomogeneous plane wave by a edge, J. Opt. Soc. Amer. 68 (7) (1978) 983–989.
[16] G. Manara, P. Nepa, R.G. Kouyoumjian, B.J.E. Taute, The diffraction of an inhomogeneous plane wave by an impedance wedge in a lossy medium, IEEE Trans. Ant. Prop. 46 (11) (1998) 1753–1755.
[17] P. Bernardi, et al., A three-dimensional UTD heuristic diffraction coefficient for complex penetrable wedges, IEEE Trans. Ant. Prop. 50 (2) (2002) 217–224.
[18] J.F. Rouvière, N. Douchin, P.F. Combes, Improvement of the UTD formulation for diffraction of an electromagnetic wave by a dielectric wedge, Electron. Lett. 33 (5) (1997) 373–375.
[19] R. Matschek, A heuristic UTD diffraction coefficient for lossy dielectric wedges including multiple internal reflections, in: PIERS 2000, Boston, USA, 2000.
[20] J. Vandamme, S. Baranowski, P. Degauque, Three dimensional modeling of double diffraction phenomena by a high building, in: IEEE VTC'96, vol. 2, pp. 1283–1287, 1996.
[21] H. Sizun, La Propagation des ondes radioélectriques, Collection Technique et Scientifique des Télécommunications, Springer-Verlag, Berlin/New York, 2002.
[22] B. Foulonneau, F. Gaudaire, Y. Gabillet, Measurement method of electromagnetic transmission loss of building components using two reverberation chambers, Electron. Lett. 22 (23) (1996) 2130–2131.
[23] J.L. Dessalles, L'ordinateur génétique, Editions Hermès.